



Synthesis, optical properties and preliminary in vitro photodynamic effect of pyridyl and quinoxalyl substituted chlorins



Jiazhu Li^{a,*}, Xin Zhang^b, Yang Liu^a, Il Yoon^c, Dong-Kyoo Kim^d, Jun-Gang Yin^a, Jin-Jun Wang^a, Young Key Shim^{c,*}

^a College of Chemistry and Chemical Engineering, Yantai University, Yantai 264005, China

^b School of Life Science and Biopharmaceutics, Shenyang Pharmaceutical University, Shenyang 110016, China

^c PDT Research Institute, School of Nano System Engineering, Inje University, Gimhae 621-749, Republic of Korea

^d Department of Biomedical Chemistry and Institute of Basic Science, Inje University, Gimhae 621-749, Republic of Korea

ARTICLE INFO

Article history:

Received 6 February 2015

Revised 7 March 2015

Accepted 8 March 2015

Available online 14 March 2015

Keywords:

Chlorophyll *a*

Pyridyl chlorin

Quinoxalyl chlorin

Photosensitizer

Photodynamic therapy

ABSTRACT

A series of chlorophyll *a*-based chlorins conjugated with pyridyl or quinoxalyl group at different positions were synthesized, characterized and evaluated for their photodynamic effect in vitro. It was found that all the pyridyl and quinoxalyl chlorins showed promising photocytotoxicities but nontoxic without irradiation in HeLa cells, and the substituted types and positions had a significant influence on the photocytotoxicities of the chlorophyll *a*-based chlorins. All the chlorins with a pyridyl group at the C–D ring end exhibited relatively high photocytotoxicity as compared to those with 3²-pyridyl. Among them, compound **12** conjugated with a pyridyl group at its C12 position showed the best photodynamic effect in HeLa cells with an IC₅₀ value of 0.033 μM. These facts, associated with the relative high long wavelength absorptions of those chlorins may provide valuable ways to design and prepare promising photosensitizers for application in photodynamic therapy.

© 2015 Elsevier Ltd. All rights reserved.

1. Introduction

Photodynamic therapy (PDT) consists of the administration and effective accumulation of a photosensitizer (PS) by target tumor tissues, followed by generation of singlet oxygen and other cytotoxic reactive oxygen species (ROS) that result in cell membrane damage and subsequent cell death upon irradiation with light of appropriate wavelength in the presence of tissue oxygen (O₂).¹ Photofrin is the first photosensitizer to receive regulatory approval for the treatment of various cancers in more than 40 countries throughout the world, including the United States (by FDA in 1995).² To overcome the drawbacks of the first generation PS Photofrin, many new generation PSs have been developed and introduced in clinical trials, most of whom are cyclic tetrapyrroles comprising substituted derivatives of porphyrin, (bacterio)chlorin and phthalocyanine.³ In recent years, PS which can easily be prepared by partial synthesis starting from abundant natural materials, such as heme, chlorophyll and bacteriochlorophyll, attracted maximum interests in that they have both economical and environmental advantages.⁴ A series of chlorophyll

a-based photosensitizers such as purpurinimide,^{5,6} HPPH,^{7–9} and NPe₆^{10–12} have been developed and are studied at various stages of preclinical or advanced clinical trials.

Due to their applications in the construction of biomimetic models of photosynthetic systems, pyridyl porphyrins or chlorins and their metal complexes have recently attracted considerable attention.^{13–15} Their water-soluble quaternary salts have also been studied comprehensively, such as monocationic cycloimide derivatives of chlorin *p*₆ (CICD),¹⁶ cationic water-soluble esters of chlorin *e*₆,^{17,18} cationic *meso*-porphyrins^{19,20} and cationic β-vinyl substituted *meso*-tetraphenylporphyrins.²¹

Based on these intriguing results, we have designed and synthesized a series of 3²-pyridyl or quinoxalyl substituted chlorins and their quaternary salts via stereoselective aldol-like carbon–carbon condensation (Fig. 1).^{22,23} Such compounds possess carbon–carbon bond linked pyridyl or quinoxalyl groups which conjugated to the chlorin macrocycle π-system via a vinyl bridge. It has been proved that their quaternary salts showed promising photodynamic effect in HeLa cells, but the photodynamic effect of 3²-pyridyl or quinoxalyl substituted chlorins is still an open question. In the present work we proposed the synthesis of a new series of pyridyl substituted chlorins which have a pyridyl group linked at the C–D ring end of the macrocycle, and the comparative study of all these

* Corresponding authors. Tel.: +86 535 6903490; fax: +86 535 6902078 (J.L.); tel.: +82 55 320 3871; fax: +82 55 320 3872 (Y.K.S.).

E-mail addresses: jiazhu82@ytu.edu.cn (J. Li), ykshim@inje.ac.kr (Y.K. Shim).

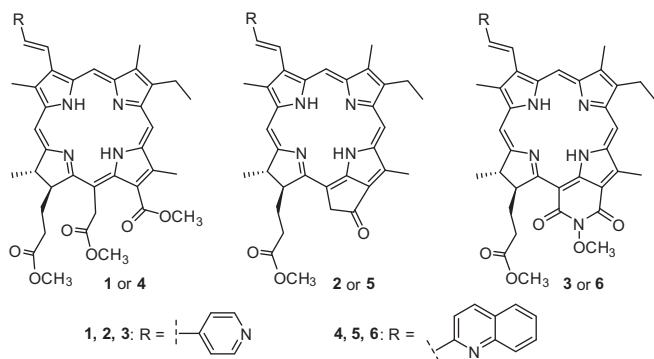


Figure 1. Structures of the 3²-pyridyl or quinoxalyl substituted chlorins **1–6** prepared via aldol-like condensation.

pyridyl or quinoxalyl chlorins about their optical properties and photodynamic activities in HeLa cells.

2. Results and discussion

2.1. Synthesis and characterization

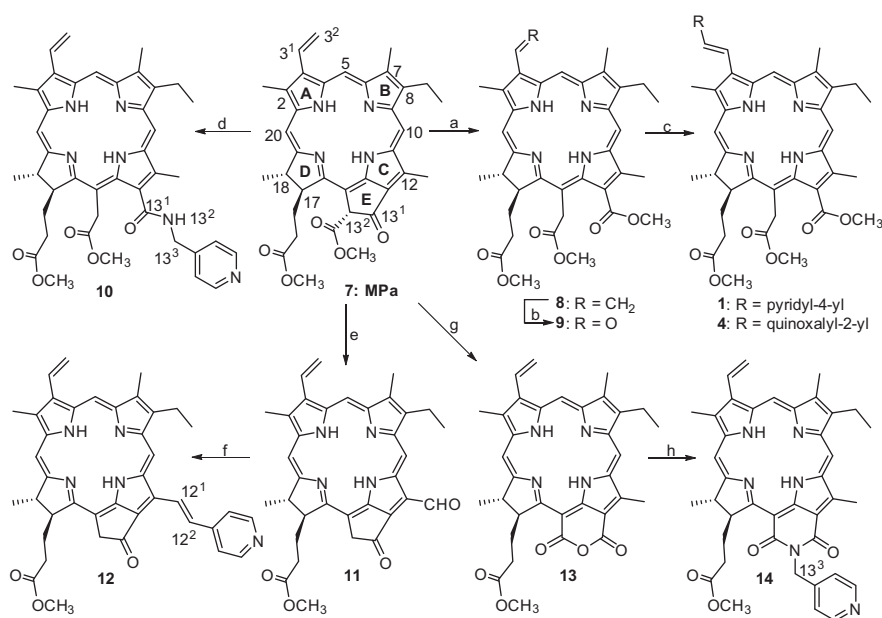
The synthesis of 3²-pyridyl or quinoxalyl substituted chlorins **1–3**, **5** and **6** has been reported previously.^{22,23} As shown in **Scheme 1**, Preparation of 3²-quinoxalyl substituted chlorin **4** was started from the ring-opening reaction of methyl pheophorbide *a* (MPa) **7** resulted in the production of chlorin *e*₆ trimethyl ester **8**, followed by OsO₄/NaIO₄ oxidation to give the 3-formyl-3-devinyl chlorin *e*₆ trimethyl ester **9**, which was refluxed with quinaldine in Ac₂O for 5 h to give the desired product **4** (*m/z* 766.4) as dark brown solid in 55% yield. In order to compare the difference of properties among chlorins with the pyridyl group at various substituted positions, a series of new pyridyl chlorins were prepared using MPa **7** as the substrate. Chlorin **10** was prepared from MPa **7** via nucleophilic substitution with 4-(aminomethyl) pyridine at its C13¹ position, the desired product **10** (*m/z* 715.4) was readily

purified by silica gel chromatography to give a dark green solid in 61% yield. While 12²-pyridyl chlorin **12** was prepared by the similar method to that of chlorin **4** from 12-formyl-12-demethyl pyropheophorbide *a* methyl ester **11**, which has been reported by Wang et al. previously.²⁴ The desired product **12** (*m/z* 638.5) was obtained as a green solid in 51% yield after silica gel chromatography. As for the preparation of pyridyl purpurinimide **14**, purpurin 18 methyl ester **13**, prepared from MPa **7** via air oxidation in alkaline solution,⁵ was refluxed with 4-(aminomethyl)pyridine in toluene under nitrogen atmosphere for 8 h to afford the desired product **14** (*m/z* 699.4) in 85% yield as purple red solid.

The structures of all the new chlorins were characterized by the ¹H NMR spectra. As shown in **Figure 2**, the 3²-pyridyl proton signals of chlorin **2** appeared as two doublets at δ 8.80 and 7.72, while its 3-vinyl proton signals showed at δ 8.60 and 7.56 as two doublets with the coupling constant (*J*) of 16.0 Hz, typical of an *E*-geometry of the double bond. In contrast, the proton signals of 4-pyridylethylene at the C12 position of chlorin **12** appeared at δ 8.77, 7.84 (two doublets, pyridyl) and δ 8.98, 8.63 (two doublets, 12-vinyl), respectively. It is worth noting that the geometry of the 12-ethylene linker is also an *E*-type based on the coupling constant (16.3 Hz). The appearance of the typical ABX system of 3-vinyl proton signals at δ 7.91 (dd), 6.26 (d), 6.17 (d) and the disappearance of the 12-CH₃ proton signal further confirmed the structure of chlorin **12**. In the ¹H NMR spectrum of chlorin **10**, the 13²-NH, 13³-CH₂ and pyridyl proton signals appeared at δ 6.70 as broad singlet, δ 4.82, 4.42 as two doublet of doublets and δ 8.51 and 7.22 as two doublets, respectively. While for the chlorin **14**, the proton signals of 13³-CH₂ was observed at δ 5.68 as a singlet, and the pyridyl proton signals appeared at δ 8.60 and 7.58 as two doublet of doublets.

2.2. Optical property

The optical properties of the pyridyl or quinoxalyl chlorins are shown in **Figure 3** and summarized in **Table 1**. In the electronic absorption spectra, it was observed that all the 3²-pyridyl or quinoxalyl chlorins **1–6** and 12²-pyridyl chlorin **12** showed a



Scheme 1. Synthetic routes of 3²-quinoxalyl substituted chlorin **4** and pyridyl chlorins **10**, **12** and **14** which have a pyridyl group linked at the C–D ring end of the macrocycles. Reaction conditions: (a) NaOMe, MeOH, 0 °C, 2 h; (b) OsO₄, NaIO₄, rt, 3 h; (c) quinaldine, Ac₂O, AcOH, reflux, 5 h; (d) 4-(aminomethyl) pyridine, rt, 12 h; (e) LiOH/H₂O/MeOH/THF, rt, 2 h; (f) 4-picoline, Ac₂O, reflux, 5 h; (g) KOH/1-propanol/pyridine/Et₂O, O₂, 1 h; (h) 4-(aminomethyl) pyridine, toluene, reflux, 8 h.

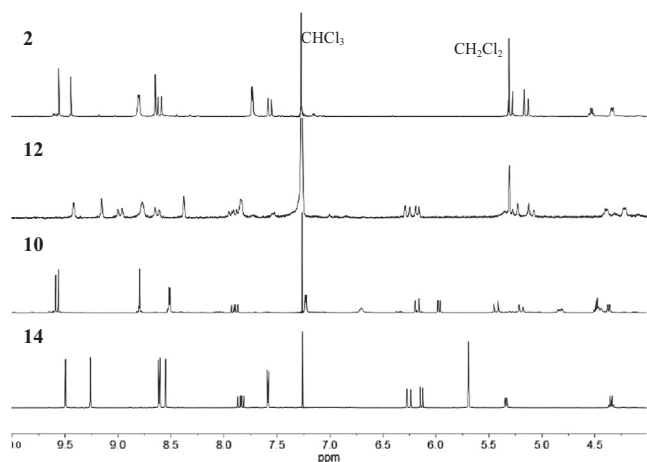


Figure 2. The comparative ^1H NMR spectra (CDCl_3 , 500 MHz) in the region δ 4.0–10.0 ppm of pyridyl substituted chlorins **2**, **10**, **12** and **14**.

bathochromic shift (10–53 nm) of their long wavelength absorption bands (Q_y bands) compared with methyl pyropheophorbide *a* (MPPa, 668 nm), which can be explained by the π -extension effect derived from the conjugated connection of the pyridyl or quinoxalyl group surrounding the periphery of chlorin macrocycle. While chlorin **10** and **14** showed typical Q_y absorptions of their precursors chlorin e_6 (663 nm) and purpurinimide (708 nm), respectively. In comparison with 3²-pyridyl chlorins **1–3** ($\Delta Q_y = 10$, 10 and 48 nm, respectively), the 3²-quinoxalyl chlorins **4–6** showed more bathochromic shift of their Q_y absorptions ($\Delta Q_y = 11$, 12 and 53 nm, respectively). It was interesting to find that the conjugated position of the pyridyl group surrounding the periphery of chlorin macrocycle has a significant influence on their electronic absorption spectra. As shown in Figure 3A, the 12²-pyridyl chlorin **12** showed not only relative high bathochromic shift of its Q_y absorption ($\Delta Q_y = 29$ nm), but also the increased absorption intensities of all the peaks including its Soret, Q_x and Q_y bands compared to 3²-pyridyl chlorin **2**. Such properties are desired for a photosensitizer in both photodynamic therapy and dye-sensitized solar cell study.²⁵ In the fluorescence spectra, these chlorins showed distinct emission bands and intensities, among them, 3²-quinoxalyl chlorin **14** showed the largest Stokes shift (9 nm).

2.3. In vitro photodynamic activity in HeLa cells

To investigate their potential in PDT, preliminary in vitro photodynamic effects of these pyridyl or quinoxalyl chlorins **1–6**, **10**, **12** and **14** were evaluated by WST-8 assay against HeLa cells exposed to increasing concentrations of each compound up to

10 μM at 12 h incubation in dark or after photoirradiation (670–710 nm light, total light dose 2 J/cm² for 15 min). As shown in Figure 4A and B, all the pyridyl or quinoxalyl chlorins showed very low dark toxicity up to the highest concentration (10 μM) investigated. However, upon exposure to a low light dose, all the compounds showed significant reduction in HeLa cell viability in a concentration-dependent manner. With an increase in the concentration of the photosensitizer, the cell viability revealed decreasing results. For example, chlorins **10** and **12** showed cell viabilities of 65.5% and 22.2% at 0.05 μM after PDT, respectively, while at 0.1 μM after PDT, their cell viabilities were changed to 28.1% and 1.4%, respectively.

Table 2 summarized the IC_{50} values of the pyridyl or quinoxalyl chlorins and the reference compound MPPa against HeLa cells after PDT. It was observed that all the tested chlorins exhibited significant photodynamic anticancer activity against HeLa cells at micro molar concentration with IC_{50} values of <5 μM . The pyridyl substituted chlorin e_6 derivatives **1**, **4**, **10** and the 12²-pyridyl substituted methyl pyropheophorbide *a* **12** showed obviously increased photodynamic activity against HeLa cells as compared to the reference compound MPPa ($\text{IC}_{50} = 0.182$ μM). Among them, chlorin **12** ($\text{IC}_{50} = 0.033$ μM) showed the best result, which increased the photodynamic activity by almost an order of magnitude in comparison with MPPa. It is interesting to observe that 3²-pyridyl or quinoxalyl substituents of different chlorin derivatives showed different effect on their phototoxicity.

As shown in Figure 4B and Table 2 and 3²-pyridyl substituted chlorin e_6 derivative **1** ($\text{IC}_{50} = 0.141$ μM) and MPPa derivative **2** ($\text{IC}_{50} = 0.581$ μM) showed relative high phototoxicity in comparison with 3²-quinoxalyl substituted derivatives **4** ($\text{IC}_{50} = 0.170$ μM) and **5** ($\text{IC}_{50} = 0.631$ μM), respectively. While for the purpurinimide-based chlorins, the 3²-quinoxalyl substituted derivative **6** ($\text{IC}_{50} = 0.992$ μM) showed better phototoxicity than 3²-pyridyl derivative **3** ($\text{IC}_{50} = 3.118$ μM). It was also observed that the different substituted positions of pyridyl group have significant influence on the phototoxicity of the chlorins. Generally speaking, chlorins **10**, **12** and **14** which have a pyridyl group linked at the C–D ring end of their macrocycles exhibited significant increased phototoxicity as compared to those have a 3²-pyridyl substituent (compounds **1–3**). For example, 13-pyridyl substituted chlorin e_6 derivative **10** and 12-pyridyl substituted MPPa **12** exhibited phototoxicity against HeLa cells at IC_{50} value of 0.071 and 0.033 μM , respectively, while the IC_{50} value of the corresponding 3²-pyridyl derivatives **1** and **2** is only 0.141 and 0.581 μM , respectively. These results suggest that the types and positions of substituents influenced significantly on the phototoxicity of chlorophyll *a*-based chlorins, and those chlorins with a pyridyl group linked at the C–D ring end are promising photosensitizers for application in photodynamic therapy.

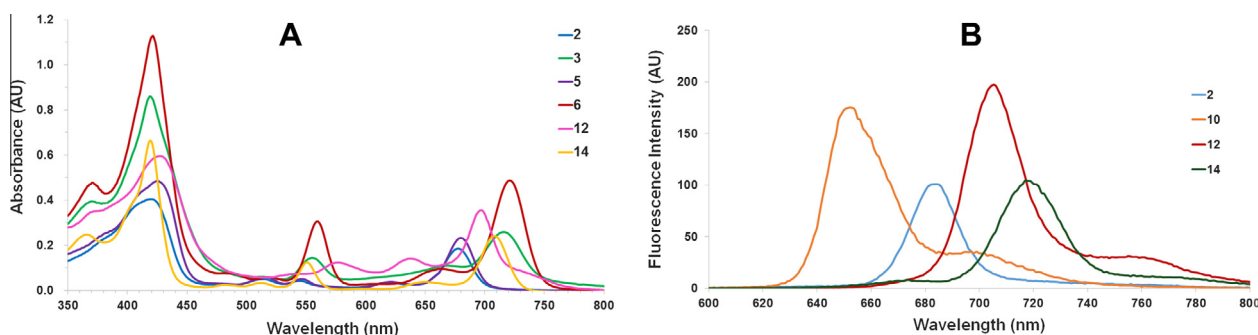


Figure 3. Comparative electronic absorption spectra (10 μM in CH_2Cl_2) of pyridyl or quinoxalyl substituted chlorins **2**, **3**, **5**, **6**, **12**, **14** (A) and fluorescence spectra (1 μM in CH_2Cl_2) of pyridyl chlorins **2**, **10**, **12** and **14** (B).

Table 1
The absorption and emission properties of the novel chlorins in dichloromethane

Compound	Absorption λ_{\max} (nm) ($\epsilon \times 10^4 \text{ M}^{-1} \text{ cm}^{-1}$)				Emission λ_{\max} (nm)		Stokes shift ^c (nm)
	Soret	ΔSoret ($\Delta\epsilon$) ^a	Q_y	ΔQ_y ($\Delta\epsilon$) ^a	Excitation	Emission	
1	412 (6.31)	-2 (-1.01)	678 (2.26)	10 (-0.95)	412	685	7
2	421 (4.05)	7 (-3.27)	678 (1.86)	10 (-1.35)	421	684	6
3	420 (8.60)	6 (1.28)	716 (2.60)	48 (-0.61)	420	723	7
4	412 (5.71)	-2 (-1.61)	679 (2.30)	11 (-0.91)	412	685	6
5	424 (4.85)	10 (-2.47)	680 (2.33)	12 (-0.88)	424	685	5
6	422 (11.27)	8 (3.95)	721 (4.88)	53 (1.67)	422	728	7
10	403 (11.61)	-11 (4.29)	663 (5.04)	-5 (1.83)	403	670	7
12	427 (5.96)	13 (-1.36)	697 (3.56)	29 (0.35)	427	705	8
14	419 (6.63)	5 (-0.69)	708 (2.42)	40 (-0.79)	419	717	9

^a ΔSoret , ΔQ_y and $\Delta\epsilon$ represent the change of the Soret band, Q_y band and absorbance intensity, respectively, between the novel chlorins and methyl pyropheophorbide **a**.²³
^c Stokes shift a longest wavelength absorption.

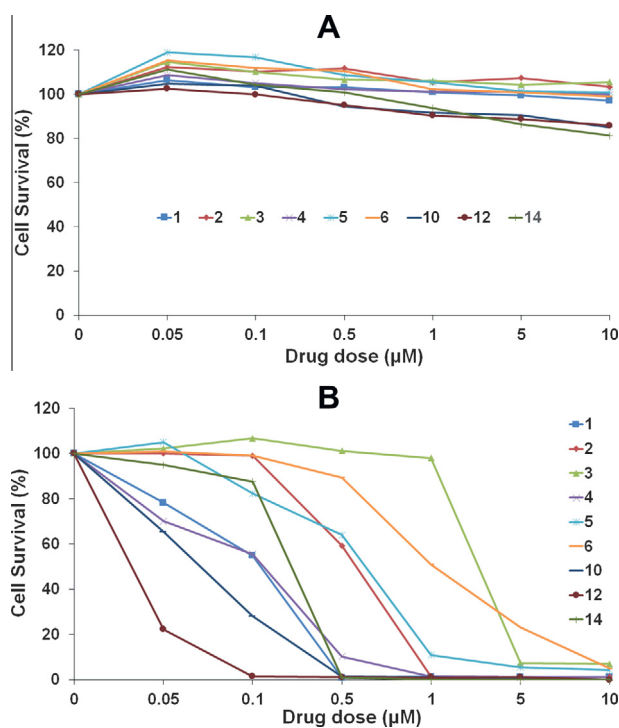


Figure 4. Cell viability results in dark (A) and after PDT (B) in HeLa cells for pyridyl or quinoxalyl substituted chlorins **1–6**, **10**, **12** and **14**. The cell viabilities of these photosensitizers after PDT were evaluated in the concentration ranges of 0–10 μM after 12 h. Surviving cell population was measured by WST-8 assay. The data are expressed as mean of three experiments.

2.4. Singlet oxygen study

In most of the photosensitizers, the formation of singlet oxygen ($^1\text{O}_2$) when the photosensitizer is exposed to light is believed to be one of the main causes of cytotoxicity. The relative difference of singlet oxygen generation of the pyridyl or quinoxalyl substituted chlorins **1–6**, **10**, **12** and **14** after photoirradiation were measured

Table 2
 IC_{50} values of photosensitizers in HeLa cells

Compound	MPPa	1	2	3	4
IC_{50}^a (μM)	0.182	0.141	0.581	3.118	0.170
Compound	5	6	10	12	14
IC_{50}^a (μM)	0.631	0.992	0.071	0.033	0.189

^a IC_{50} represents the half maximal (50%) inhibitory concentration of the photosensitizers.

by the $^1\text{O}_2$ -induced bleaching of 1,3-diphenylisobenzofuran (DPBF) using methylene blue (MB) as the reference compound.^{26,27} As shown in Figure 5, all the pyridyl or quinoxalyl substituted chlorins produced $^1\text{O}_2$ efficiently after photoirradiation. Among them, 12²-pyridyl substituted MPPa **12** exhibited the best result of $^1\text{O}_2$ generation, which is correlated well with the phototoxicity study, while it should be noted that the $^1\text{O}_2$ generation order of these chlorins is not correlated with their phototoxicities against HeLa cells.

2.5. The hydrophobic property study

It is generally well established that the hydrophobic property of the chlorophyll *a*-based photosensitizers play a significant role in their photosensitizing efficacy and is closely related to their cellular uptake property.²⁸ The hydrophobicity parameter ($\log P$) of the pyridyl or quinoxalyl substituted chlorins **1–6**, **10**, **12** and **14** were calculated by a program module of the ACD/Labs software (version 14.02, Advanced Chemistry Development, Inc., Toronto, ON, Canada). As shown in Table 3, all the pyridyl or quinoxalyl substituted chlorins have $\log P$ values in the range of 6.0–10.0. It is

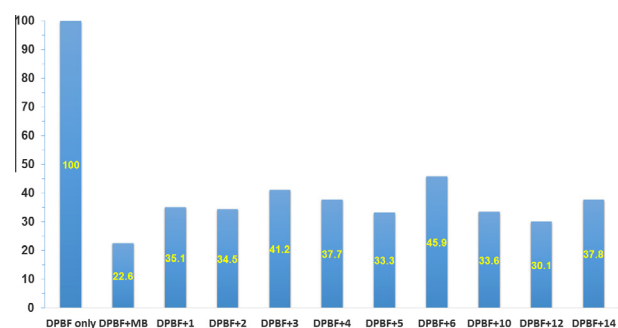


Figure 5. Comparative absorbance decay (%) of 1,3-diphenylisobenzofuran (DPBF, 50 μM in DMSO) at 418 nm after photoirradiation in the absence (control) and presence of 1 μM methylene blue (MB), compounds **1–6**, **10**, **12** and **14**, respectively. The data are expressed as mean of three experiments.

Table 3
Hydrophobicity parameters ($\log P$) of photosensitizers calculated by means of ACD/Labs (version 14.02)

Compound	$\log P$	Compound	$\log P$
1	8.45 \pm 1.64	6	8.27 \pm 1.65
2	8.31 \pm 1.61	10	7.07 \pm 1.65
3	6.92 \pm 1.65	12	8.33 \pm 1.61
4	9.81 \pm 1.64	14	6.11 \pm 1.65
5	9.67 \pm 1.61		

interesting to find that the chlorins **10**, **12** and **14** which have a pyridyl group linked at the C–D ring end of their macrocycles showed relative low log*P* values as compared to 3²-pyridyl or quinoxalyl substituted chlorins **1–6**. While as shown in the in vitro study, chlorins **10**, **12** and **14** exhibited better phototoxicity than compounds **1–6**, which might be suggested that a lower hydrophobicity of this kind of photosensitizers is desirable for the photosensitizing efficacy against HeLa cells.

3. Experimental section

3.1. General information

All reactions were monitored by TLC using 0.20 mm silica gel plates with or without UV indicator (60F-254). Silica gel 60 (230–400 mesh, Merck) was used for flash column chromatography. ¹H NMR spectra were measured at 500 MHz on a Bruker Advance II spectrometer. Chemical shifts (δ) are given in ppm relative to tetramethylsilane (TMS, 0 ppm) unless otherwise indicated. Electronic absorption spectra were measured on a AOE A560 UV–Vis spectrophotometer. The absorption maxima λ_{\max} are given in nm and molar absorbance coefficient (ϵ) or relative intensity. The fluorescence spectra were measured on a Varian Cary Eclipse fluorescence spectrophotometer. FABMS and HRMS were obtained on a Jeol JMS700 high resolution mass spectrometer at the Korea Basic Science Institute (Daegu). Materials obtained from commercial suppliers were used without further purification. Chlorins **1–3**, **5** and **6** have been reported by us previously.^{22,23} Methyl pheophorbide **a** **7** was prepared according to the procedure described in the literature.²⁹

3.2. Synthesis and characterization of new compounds

3.2.1. Synthesis of 3-formyl-3-devinyl chlorin *e*₆ trimethyl ester (**9**)

Chlorin *e*₆ trimethyl ester **8** was prepared from methyl pheophorbide **a** **7** as previously reported,¹¹ and its spectroscopic characterization agreed fully with the published data. To a solution of chlorin *e*₆ trimethyl ester **8** (210 mg, 0.329 mmol) in 80 mL THF were added a solution of OsO₄ (10 mg) in CCl₄ (20 mL) and a solution of NaIO₄ (2.0 g, 9.35 mmol) in water (50 mL) successively. The mixture was stirred violently at room temperature for 3 h. It was then diluted with CH₂Cl₂ (150 mL), washed with water (3 × 150 mL), and dried over anhydrous Na₂SO₄. The organic phase was evaporated and the residue was purified on a silica gel column eluting with ethyl acetate/*n*-hexane (1:1). After the major dark brown band was eluted from the column, the solvent was evaporated to yield 188 mg (0.293 mmol, 89%) of the title compound **9** as dark brown solid. UV–vis (CH₂Cl₂) λ_{\max} ($\epsilon \times 10^4$): 421 (7.42), 513 (0.54), 546 (0.60), 666 (0.93), 693 (1.91) nm. ¹H NMR (500 MHz, CDCl₃) δ 11.40 (s, 1H, 3¹-H), 10.62 (s, 1H, 10-H), 9.99 (s, 1H, 5-H), 9.37 (s, 1H, 20-H), 5.48 (d, *J* = 19.1 Hz, 1H, 15¹-H), 5.43 (d, *J* = 19.4 Hz, 1H, 15¹-H), 4.68 (q, *J* = 7.3 Hz, 1H, 18-H), 4.58 (dd, *J* = 11.0, 2.2 Hz, 1H, 17-H), 3.90 (q, *J* = 7.5 Hz, 2H, 8¹-CH₂), 4.30, 3.86, 3.84, 3.74, 3.64, 3.42 (each s, each 3H, CH₃ + OCH₃), 2.78–2.68, 2.49–2.40, 2.22–2.12 (each m, total 4H, 17¹ + 17²-CH₂), 1.90 (d, *J* = 7.3 Hz, 3H, 18-CH₃), 1.66 (t, *J* = 7.7 Hz, 3H, 8²-CH₃), –1.03, –1.70 (each br s, each 1H, NH). Anal. Calcd for C₃₆H₄₀N₄O₇: C, 67.48; H, 6.29; N, 8.74. Found: C, 67.54; H, 6.31; N, 8.75.

3.2.2. Synthesis of (*E*)-3²-(quinoline-2-yl) chlorin *e*₆ trimethyl ester (**4**)

Compound **9** (150 mg, 0.234 mmol) and quinaldine (0.1 mL) were refluxed in acetic anhydride (10 mL) with one drop of acetic

acid under nitrogen atmosphere for 5 h. The reaction mixture was evaporated to remove the solvent, and the residue was dissolved in dichloromethane (30 mL), washed with 1 M aqueous HCl (3 × 50 mL), then with water (2 × 50 mL). The organic layer obtained was dried over anhydrous Na₂SO₄, concentrated, and purified on a silica gel column using acetone/dichloromethane (2%–5%) as gradient eluent to yield 99 mg (0.129 mmol, 55%) of the title product **4** as dark brown solid. UV–vis (CH₂Cl₂) λ_{\max} ($\epsilon \times 10^4$): 412 (5.71), 504 (0.82), 541 (0.72), 629 (0.52), 678 (2.30) nm. ¹H NMR (500 MHz, CDCl₃) δ 9.74 (s, 1H, 10-H), 9.70 (s, 1H, 5-H), 9.14 (d, *J* = 16.3 Hz, 1H, 3¹-H), 8.83 (s, 1H, 20-H), 8.32 (d, *J* = 8.4 Hz, 1H, 3²-H), 8.28 (d, *J* = 8.3 Hz, 1H, 6¹-H), 8.00 (d, *J* = 16.5 Hz, 1H, 3²-H), 7.99 (d, *J* = 8.5 Hz, 1H, 9¹-H), 7.91 (d, *J* = 8.1 Hz, 1H, 4¹-H), 7.82 (ddd, *J* = 8.3, 6.9, 1.4 Hz, 1H, 7¹-H), 7.60 (ddd, *J* = 8.0, 6.9, 1.1 Hz, 1H, 8¹-H), 5.36 (d, *J* = 18.9 Hz, 1H, 15¹-H), 5.25 (d, *J* = 19.0 Hz, 1H, 15¹-H), 4.47 (q, *J* = 7.2 Hz, 1H, 18-H), 4.44–4.39 (m, 1H, 17-H), 3.80 (q, *J* = 7.5 Hz, 2H, 8¹-CH₂), 4.26, 3.77, 3.65, 3.64, 3.58, 3.34 (each s, each 3H, CH₃ + OCH₃), 2.63–2.53, 2.27–2.17, 2.07–1.99 (each m, total 4H, 17¹ + 17²-CH₂), 1.76 (d, *J* = 7.3 Hz, 3H, 18-CH₃), 1.72 (t, *J* = 7.7 Hz, 3H, 8²-CH₃), –1.24, –1.49 (each br s, each 1H, NH). Anal. Calcd for C₄₆H₄₇N₅O₆: C, 72.14; H, 6.19; N, 9.14. Found: C, 72.15; H, 6.21; N, 9.17. MS (FAB) *m/z* 766.4 (MH⁺, 100). HRMS (FAB): Calcd for C₄₆H₄₈N₅O₆ (MH⁺) 766.3605; Found 766.3608.

3.2.3. Synthesis of chlorin *e*₆-13¹-*N*-(pyridine-4-yl methylene) amide-15²,17³-dimethyl ester (**10**)

A solution of methyl pheophorbide **a** **7** (200 mg, 0.330 mmol) in chloroform (10 mL) was stirred with 4-aminomethyl pyridine (0.5 mL, excess) at room temperature under nitrogen atmosphere until the disappearance of the starting material (TLC, 12 h). The reaction mixture was diluted with dichloromethane (100 mL), washed with water (3 × 100 mL), dried over anhydrous Na₂SO₄ and evaporated to dryness at 30–40 °C under reduced pressure. After purification on a silica gel column using 20% MeOH in CH₂Cl₂ as eluent to yield 144 mg (0.201 mmol, 61%) of pure product **10** as dark green solid. UV–vis (CH₂Cl₂) λ_{\max} ($\epsilon \times 10^4$): 403 (11.61), 501 (1.22), 529 (0.33), 609 (0.41), 663 (5.04) nm. ¹H NMR (500 MHz, CDCl₃) δ 9.58 (s, 1H, 10-H), 9.56 (s, 1H, 5-H), 8.79 (s, 1H, 20-H), 8.51 (dd, *J* = 4.5, 1.4 Hz, 2H, 2',6'-H), 7.89 (dd, *J* = 17.8, 11.5 Hz, 1H, 3¹-H), 7.22 (d, *J* = 5.4 Hz, 2H, 3' + 5'-H), 6.70 (s, 1H, 13²-NH), 6.17 (dd, *J* = 17.9, 1.1 Hz, 1H, 3²-H), 5.96 (dd, *J* = 11.5, 1.1 Hz, 1H, 3²-H), 5.42 (d, *J* = 19.0 Hz, 1H, 15¹-H), 5.19 (d, *J* = 19.0 Hz, 1H, 15¹-H), 4.82 (dd, *J* = 14.9, 6.2 Hz, 1H, 13³-H), 4.47 (q, 1H, 18-H), 4.42 (dd, *J* = 14.9, 6.2 Hz, 1H, 13³-H), 4.36 (dd, *J* = 10.0, 2.1 Hz, 1H, 17-H), 3.77 (q, *J* = 7.7 Hz, 2H, 8¹-CH₂), 3.70, 3.61, 3.35, 3.32, 3.28 (each s, each 3H, OCH₃ + CH₃), 2.61–2.52, 2.25–2.13, 1.83–1.76 (each m, total 4H, 17¹ + 17²-CH₂), 1.74 (d, *J* = 7.3 Hz, 3H, 18-CH₃), 1.71 (t, *J* = 7.7 Hz, 3H, 8²-CH₃), –1.61, –1.84 (each br s, each 1H, NH). Anal. Calcd for C₄₂H₄₆N₆O₅: C, 70.57; H, 6.49; N, 11.76. Found: C, 70.60; H, 6.51; N, 11.85. MS (FAB) *m/z* 715.4 (MH⁺, 100). HRMS (FAB): Calcd for C₄₂H₄₇N₆O₅ (MH⁺) 715.3563; Found 715.3605.

3.2.4. Synthesis of 12-formyl-12-demethyl pyropheophorbide *a* methyl ester (**11**)

Methyl pheophorbide **a** **7** was transformed to methyl pyropheophorbide **a** (MPPa) by the method described in the literature.²⁹ To a solution of methyl pyropheophorbide **a** (550 mg, 1.00 mmol) in 50 mL THF was added 1.5 g Lithium hydroxide (dissolved in 10 mL water and 25 mL methanol). The mixture was stirred vigorously for 1 h in an open flask. The reaction mixture was then diluted with water (100 mL) and acidified to pH 3 by adding aqueous HCl (5%). It was then extracted with dichloromethane (2 × 100 mL), the organic layer was separated and washed with water (100 mL), dried over anhydrous Na₂SO₄ and evaporated to

dryness. The residue was dissolved in dichloromethane and treated with diazomethane to convert the carboxylic acid back to methyl ester. After chromatographic purification on a silica gel column with 1–4% acetone/dichloromethane as gradient eluent, the brown band and green band was collected. The title product **11** (a green solid) was obtained as minor product in 17% yield, and its spectroscopic characterization agreed fully with the published data.²⁴

3.2.5. Synthesis of 12-demethyl-12-(pyridine-4-yl ethylene)pyrphosphoribide α methyl ester (**12**)

Compound **11** (150 mg, 0.267 mmol) and 4-picoline (0.1 mL) were refluxed in acetic anhydride (10 mL) under nitrogen atmosphere for 5 h. The reaction mixture was evaporated to remove the solvent, and the residue was dissolved in dichloromethane (30 mL), washed with 1 M aqueous HCl (3 \times 50 mL), then with water (2 \times 50 mL). The organic layer obtained was dried over anhydrous Na₂SO₄, concentrated, and purified on a silica gel column using acetone/dichloromethane (2–5%) as gradient eluent to yield 87 mg (0.136 mmol, 51%) of the title product **12** as green solid. UV–vis (CH₂Cl₂) λ_{max} ($\epsilon \times 10^4$): 427 (5.96), 576 (1.23), 638 (1.41), 697 (3.56) nm. ¹H NMR (500 MHz, CDCl₃) δ 9.41 (s, 1H, 10-H), 9.15 (s, 1H, 5-H), 8.98 (d, $J = 16.3$ Hz, 1H, 12¹-H), 8.77 (m, 2H, 2' + 6'-H), 8.63 (d, $J = 16.3$ Hz, 1H, 12²-H), 8.37 (s, 1H, 20-H), 7.91 (dd, $J = 18.1, 11.4$ Hz, 1H, 3¹-H), 7.84 (m, 2H, 3' + 5'-H), 6.26 (d, $J = 18.6$ Hz, 1H, 3²-H), 6.17 (d, $J = 10.9$ Hz, 1H, 3²-H), 5.25 (d, $J = 20.2$ Hz, 1H, 13²-H), 5.10 (d, $J = 20.3$ Hz, 1H, 13²-H), 4.45–4.33 (m, 1H, 18-H), 4.25–4.17 (m, 1H, 17-H), 3.64 (q, $J = 7.4$ Hz, 2H, 8¹-CH₂), 3.63, 3.33, 3.18 (each s, each 3H, CH₃ + OCH₃), 2.75–2.52, 2.39–2.24 (each m, total 4H, 17¹ + 17²-CH₂), 1.79 (d, $J = 7.1$ Hz, 3H, 18-CH₃), 1.67 (t, $J = 7.7$ Hz, 3H, 8²-CH₃), 0.07, -0.72 (each br s, each 1H, NH). Anal. Calcd for C₄₀H₃₉N₅O₃: C, 75.33; H, 6.16; N, 10.98. Found: C, 75.41; H, 6.19; N, 10.94. MS (ESI) m/z 638.5 (MH⁺, 100).

3.2.6. Synthesis of purpurin 18 methyl ester (**13**)

Purpurin 18 methyl ester **13** was prepared from methyl pheophorbide **a** **7** by air oxidation in alkaline solution as previously published, and its spectroscopic characterization agreed with the published data.^{5,30}

3.2.7. Synthesis of purpurin-18-N-(pyridine-4-yl methylene)imide methyl ester (**14**)

Purpurin 18 methyl ester **13** (200 mg, 0.346 mmol) and 4-aminomethyl pyridine (0.2 mL, excess) were refluxed in anhydrous toluene (10 mL) for 8 h under a nitrogen atmosphere. The reaction was monitored periodically by UV–vis spectroscopy, the disappearance of a peak at 698 nm (for the anhydride) and the appearance of a new peak at 708 nm (for the purpurinimide) indicated completion of the reaction. After evaporating the solvents from the reaction mixture, the crude material was dissolved in dichloromethane (50 mL) and washed with water (3 \times 50 mL), organic layer obtained was dried over anhydrous Na₂SO₄, concentrated, and purified over a silica gel column using ethyl acetate/*n*-hexane (1:1) as eluent to yield 197 mg (0.295 mmol, 85%) of pure product **14** as purple red solid. UV–vis (CH₂Cl₂) λ_{max} ($\epsilon \times 10^4$): 419 (6.63), 481 (0.26), 511 (0.33), 551 (1.25), 649 (0.38), 708 (2.42) nm. ¹H NMR (500 MHz, CDCl₃) δ 9.49 (s, 1H, 10-H), 9.25 (s, 1H, 5-H), 8.60 (dd, $J = 4.6, 1.6$ Hz, 2H, 2' + 6'-H), 8.54 (s, 1H, 20-H), 7.83 (dd, $J = 17.8, 11.5$ Hz, 1H, 3¹-H), 7.58 (dd, $J = 4.7, 1.6$ Hz, 2H, 3' + 5'-H), 6.25 (dd, $J = 17.8, 1.2$ Hz, 1H, 3²-H), 6.13 (dd, $J = 11.5, 1.2$ Hz, 1H, 3²-H), 5.68 (s, 2H, 13³-CH₂), 5.33 (dd, $J = 9.1, 2.2$ Hz, 1H, 17-H), 4.34 (q, $J = 7.4$ Hz, 1H, 18-H), 3.54 (q, $J = 7.7$ Hz, 2H, 8¹-CH₂), 3.75, 3.54, 3.32, 3.08 (each s, each 3H, OCH₃ + CH₃), 2.73–2.64, 2.43–2.33, 2.00–1.93 (each m, total 4H, 17¹ + 17²-CH₂), 1.76 (d, $J = 7.4$ Hz, 3H, 18-CH₃), 1.61 (t, $J = 7.7$ Hz, 3H, 8²-CH₃), 0.05, -0.08 (each br s, each 1H, NH). Anal. Calcd for

C₄₀H₄₀N₆O₄: C, 71.84; H, 6.03; N, 12.57. Found: C, 71.81; H, 6.07; N, 12.62. MS (FAB) m/z 669.3 (MH⁺, 100). HRMS (FAB): Calcd for C₄₀H₄₁N₆O₄ (MH⁺) 669.3189; Found 669.3186.

3.3. In vitro photosensitizing efficacy against HeLa cells

The photodynamic effect of the selected photosensitizers on cell viability was investigated in HeLa cell line. The HeLa cells obtained from American Type Culture Collection (ATCC) were cultured in EMEM medium supplemented with 10% FBS at 37 °C (5% CO₂) in a humidified atmosphere. Cells were plated at 5 \times 10³ cells into each well of a 96-well microplate. After 24 h of incubation, media were substituted by fresh media containing photosensitizers at various concentrations. Plates were returned to the incubator for 24 h. And then the cells were replaced with fresh media and exposed to light (BioSpec LED, 670–710 nm, 2.0 J/cm²) for 15 min (for the determination of the dark toxicity, to skip over this step and incubate for 12 h directly). Following illumination, the plates were incubated further for 12 h at 37 °C in the dark. CCK-8 reagent (10 μ L) was then added to each well followed by 2 h incubation. The cell viability was assessed by WST-8 [2-(2-methoxy-4-nitrophenyl)-3-(4-nitrophenyl)-5-(2,4-disulfophenyl)-2H-tetrazolium], an indicator that is reduced by dehydrogenases in cells to give an orange colored product (formazan), which is soluble in cell culture medium. The optical density for living cells was read at 450 nm in a multi-microplate reader (synergy HT, BIO-TEK[®]). Wells containing cells and an appropriate volume of the vehicle (DMSO) served as the control. Wells containing only culture medium and CCK-8 reagent served as the blank. Each experiment was repeated at least three times.

3.4. Measurement of singlet oxygen generation

The relative difference of singlet oxygen generation of the pyridyl or quinoxalyl substituted chlorins **1–6**, **10**, **12** and **14** after photoirradiation were measured using 1,3-diphenylisobenzofuran (DPBF) as the selective ¹O₂ acceptor, and methylene blue (MB) as the reference compound. A solution of DPBF (50 μ M) in DMSO was prepared as control sample, and sample solutions of DPBF (50 μ M) with 1 μ M methylene blue (reference compound), chlorins **1–6**, **10**, **12** and **14**, respectively in DMSO were prepared in dark. All the samples were placed in a 96-well plate and the container was covered with aluminum foil. The samples were irradiated (2 J/cm²) for 15 min. After irradiation, visible spectra of the sample solutions were measured spectrometrically. The normalized absorbance of DPBF at 418 nm in these samples were reported. The ¹O₂ photogeneration activities of MB, chlorins **1–6**, **10**, **12** and **14** can be compared with the different absorbance decay of each sample relative to the DPBF control sample.

4. Conclusions

In conclusion, three new chlorins **10**, **12** and **14** with a pyridyl group linked at the C-D ring end of their macrocycles have been synthesized in good to excellent yields through simple synthetic approaches. These chlorins, as well as the 3²-substituted derivatives **1–6** were studied comparatively for their optical properties and in vitro photosensitizing efficacies against HeLa cells. All of the chlorins showed high photocytotoxic activity in HeLa cell line, it was found that the types and positions of substituents influenced significantly on the phototoxicity of chlorophyll *a*-based chlorins, and those chlorins with a pyridyl group linked at the C–D ring end generally showed better phototoxicity than others. Among them, chlorin **12** had the highest efficacy at lower concentration, which increased the photodynamic activity by almost an order of

magnitude in comparison with MPPa. These facts, associated with their relative high long wavelength absorptions may provide valuable ways to design and prepare promising photosensitizers for application in photodynamic therapy. Further in vitro and in vivo studies concerning the cellular uptake, intracellular localization and the mechanism of cell death are presently in progress in our laboratory.

Acknowledgments

This work was supported by the BK21 PLUS Project and the Doctoral Science Foundation of Yantai University (HY13B11 to J.L.)

References and notes

1. Dougherty, T. J.; Gomer, C. J.; Henderson, B. W.; Jori, G.; Kessel, D.; Korbelik, M.; Moan, J.; Peng, Q. *J. Natl Cancer Inst.* **1998**, *90*, 889.
2. Dolmans, D. E.; Fukumura, D.; Jain, R. K. *Nat. Rev. Cancer* **2003**, *3*, 380.
3. Ethirajan, M.; Chen, Y. H.; Joshi, P.; Pandey, R. K. *Chem. Soc. Rev.* **2011**, *40*, 340.
4. Pandey, R. K.; Goswami, L. N.; Chen, Y.; Gryshuk, A.; Missert, J. R.; Oseroff, A.; Dougherty, T. J. *Lasers Surg. Med.* **2006**, *38*, 445.
5. Zheng, G.; Potter, W. R.; Camacho, S. H.; Missert, J. R.; Wang, G. S.; Bellnier, D. A.; Henderson, B. W.; Rodgers, M. A. J.; Dougherty, T. J.; Pandey, R. K. *J. Med. Chem.* **2001**, *44*, 1540.
6. Williams, M. P. A.; Ethirajan, M.; Ohkubo, K.; Chen, P.; Pera, P.; Morgan, J.; White, W. H.; Shibata, M.; Fukuzumi, S.; Kadish, K. M.; Pandey, R. K. *Bioconjugate Chem.* **2011**, *22*, 2283.
7. Loewen, G. M.; Pandey, R.; Bellnier, D.; Henderson, B.; Dougherty, T. *Lasers Surg. Med.* **2006**, *38*, 364.
8. Bellnier, D. A.; Greco, W. R.; Loewen, G. M.; Nava, H.; Oseroff, A. R.; Dougherty, T. J. *Lasers Surg. Med.* **2006**, *38*, 439.
9. Chen, Y.; Miclea, R.; Srikrishnan, T.; Balasubramanian, S.; Dougherty, T. J.; Pandey, R. K. *Bioorg. Med. Chem. Lett.* **2005**, *15*, 3189.
10. Ferrario, A.; Kessel, D.; Gomer, C. J. *Cancer Res.* **1992**, *52*, 2890.
11. Hargus, J. A.; Fronczek, F. R.; Graca, M.; Vicente, H.; Smith, K. M. *Photochem. Photobiol.* **2007**, *83*, 1006.
12. Jinadasa, R. G. W.; Hu, X. K.; Vicente, M. G. H.; Smith, K. M. *J. Med. Chem.* **2011**, *54*, 7464.
13. Gryko, D. T.; Tasiar, M. *Tetrahedron Lett.* **2003**, *44*, 3317.
14. Rui, X.; Zha, Q.-Z.; Wei, T.-T.; Xie, Y.-S. *Inorg. Chem. Commun.* **2014**, *48*, 111.
15. Rowland, G. B.; Barnett, K.; DuPont, J. I.; Akurathi, G.; Le, V. H.; Lewis, E. A. *Bioorg. Med. Chem.* **2013**, *21*, 7515.
16. Nazarova, A.; Ignatova, A.; Feofanov, A.; Karmakova, T.; Pljutinskaya, A.; Mass, O.; Grin, M.; Yakubovskaya, R.; Mironov, A.; Maurizot, J. C. *Photochem. Photobiol. Sci.* **2007**, *6*, 1184.
17. Taima, H.; Okubo, A.; Yoshioka, N.; Inoue, H. *Tetrahedron Lett.* **2005**, *46*, 4161.
18. Taima, H.; Okubo, A.; Yoshioka, N.; Inoue, H. *Chem. Eur. J.* **2006**, *12*, 6331.
19. Schastak, S.; Jean, B.; Handzel, R.; Kostenich, G.; Hermann, R.; Sack, U.; Orenstein, A.; Wang, Y. S.; Wiedemann, P. J. *Photochem. Photobiol., B* **2005**, *78*, 203.
20. Ricchelli, F.; Franchi, L.; Miotto, G.; Borsetto, L.; Gobbo, S.; Nikolov, P.; Bommer, J. C.; Reddi, E. *Int. J. Biochem. Cell Biol.* **2005**, *37*, 306.
21. Silva, E. M. P.; Ramos, C. I. V.; Pereira, P. M. R.; Giuntini, F.; Faustino, M. A. F.; Tomé, J. P. C.; Tomé, A. C.; Silva, A. M. S.; Santana-Marques, M. G.; Neves, M. G. P. M. S.; Cavaleiro, J. A. S. J. *Porphy. Phthalocya.* **2012**, *16*, 101.
22. Li, J.-Z.; Cui, B.-C.; Wang, J.-J.; Shim, Y.-K. *Kor. Chem. Soc.* **2011**, *32*, 2465.
23. Li, J. Z.; Wang, J. J.; Yoon, I.; Cui, B. C.; Shim, Y. K. *Bioorg. Med. Chem. Lett.* **2012**, *22*, 1846.
24. Wang, J.-J.; Wang, P.; Li, J.-Z.; Jakus, J.; Shim, Y.-K. *Kor. Chem. Soc.* **2011**, *32*, 3473.
25. Li, J.; Liu, Y.; Xu, X.-S.; Li, Y.-L.; Zhang, S.-G.; Yoon, I.; Shim, Y. K.; Wang, J.-J.; Yin, J.-G. *Org. Biomol. Chem.* **2015**, *13*, 1992.
26. Wang, K.; Poon, C. T.; Choi, C. Y.; Wong, W.-K.; Kwong, D. W. J.; Yu, F. Q.; Zhang, H.; Li, Z. Y. *J. Porphy. Phthalocya.* **2012**, *16*, 85.
27. Cui, B. C.; Yoon, I.; Li, J. Z.; Lee, W. K.; Shim, Y. K. *Int. J. Mol. Sci.* **2014**, *15*, 8091.
28. Rosenfeld, A.; Morgan, J.; Goswami, L. N.; Hulchanskyy, T.; Zheng, X.; Prasad, P. N.; Seroff, A.; Pandey, R. K. *Photochem. Photobiol.* **2006**, *82*, 626.
29. Smith, K. M.; Goff, D. A.; Simpson, D. J. *J. Am. Chem. Soc.* **1985**, *107*, 4946.
30. Li, J.; Zhang, P.; Yao, N.-N.; Zhao, L.-L.; Wang, J.-J.; Shim, Y. K. *Tetrahedron Lett.* **2014**, *55*, 1086.